LBL-17367
UC-94c

Lawrence Berkeley Laboratory
UNIVERSITY OF CALIFORNIA

APPLIED SCIENCE DIVISION

RECEIVED
LAWRENCE
BERKELEY LABORATORY

APR 17 1984

LIBRARY AND
DOCUMENTS SECTION

TRANSPORT PHENOMENA IN IMPROVED ELECTROCHEMICAL CELL DESIGN FOR THE PRODUCTION OF MAGNESIUM
Final Report

D.R. Sadoway

September 1983

TWO-WEEK LOAN COPY
This is a Library Circulating Copy which may be borrowed for two weeks. For a personal retention copy, call Tech. Info. Division, Ext. 6782.

APPLIED SCIENCE DIVISION

LBL-17367 c.2

Prepared for the U.S. Department of Energy under Contract DE-AC03-76SF00098

DISCLAIMER

This document was prepared as an account of work sponsored by the United States Government. While this document is believed to contain correct information, neither the United States Government nor any agency thereof, nor the Regents of the University of California, nor any of their employees, makes any warranty, express or implied, or assumes any legal responsibility for the accuracy, completeness, or usefulness of any information, apparatus, product, or process disclosed, or represents that its use would not infringe privately owned rights. Reference herein to any specific commercial product, process, or service by its trade name, trademark, manufacturer, or otherwise, does not necessarily constitute or imply its endorsement, recommendation, or favoring by the United States Government or any agency thereof, or the Regents of the University of California. The views and opinions of authors expressed herein do not necessarily state or reflect those of the United States Government or any agency thereof or the Regents of the University of California.

LBL-17367

Transport Phenomena in Improved Electrochemical Cell Design for the Production of Magnesium*

Final Report

September 1983

submitted by:

Donald R. Sadoway, Principal Investigator
Associate Professor of Materials Engineering
Massachusetts Institute of Technology
77 Massachusetts Avenue
Cambridge, MA 02139

submitted to:

The U.S. Department of Energy
Berkeley Electrochemical Research Center
Lawrence Berkeley Laboratory
University of California
Berkeley, California 94720

* This work was supported by the Assistant Secretary for Conservation and Renewable Energy, Office of Energy Storage Systems Research, Energy Storage Division of the U.S. Department of Energy, under Contract No. DE-AC03-SF00098 and DE-AC02-81CE90033.

TABLE OF CONTENTS

I. Introduction 2

II. Experimental Program 5

A. Preparation of Electrolyte 5

B. Electrochemical and Optical Equipment. 9

III. Experimental Procedure 10

IV. Results and Discussion 12

A. Uncontaminated Electrolyte 12

B. Electrolyte with Boron Contamination 20

C. Electrolyte with Sulfur Contamination. 27

V. Conclusions. 34

List of Publications 37

Evaluation of Progress 38

Appendix 39

Bibliography 41

ABSTRACT

A laboratory scale electrolysis cell that is representative of industrial conditions has been constructed to permit visual observation within. Experiments were conducted using an electrolyte with the composition of 10% $MgCl_2$, 10% $CaCl_2$, 20% KCl, 60% NaCl, at the current densities of 5.55, 27.75, and 83.25 mA/cm^2. The effects of electrolyte contamination by 0.05% boron and 0.5% sulfur were studied by repeating the electrolyses with the addition of B_2O_3 and $MgSO_4$, respectively. The cathodic films deposited under these conditions were analyzed to determine how these impurities degrade cell performance.

With electrolytes contaminated with either boron or sulfur, galvanostatic electrodeposition occurred at voltages too low to produce magnesium metal. Instead, what appeared to be nonmetallic deposits plated out on the cathode. These deposits consisted of magnesium compounds of the contaminants. Sodium levels high enough to be consistent with possible codeposition of sodium were detected.

I. INTRODUCTION

The electrometallurgical industries in the USA and Canada are estimated to consume 5% of total generated electrical energy[1]. The electrowinning of alumium consumes the major portion of this (70%), followed by chloro-alkali processes (22%). The remaining 7-8% is accounted for by hydro-metallurgical processes. Thus, ever since the 1973-74 energy crisis, with the subsequent rapid escalation of fuel costs, the growing challenge to the above industries has been to improve upon the operating energy efficiencies of their processes.

The case of the magnesium production industry is of particular interest in this context. It has long been established that substantial savings in net energy consumption could result from incorporating magnesium in a larger way in transportation vehicles[2,3,4]. However, thus far, the relatively lower prices of other low density materials, especially aluminum, have prevented the widespread use of magnesium in this application.

In 1979, Kenney had determined that an automotive market for magnesium at nearly double the then level of the total domestic magnesium consumption already existed[5].

By 1980, Flemings et al. had perceived the potential for substantial reduction in the price of magnesium, both by innovation in the production technology, and by significant change in the structure of the magnesium marketplace, which they predicted would be accomplished by 1985 [6]. It is quite evident that with the current economic situation in the domestic metals and automotive industries, the 1985 target date is too optimistic and should be moved farther into the future.

In 1981, Flemings et al. at MIT assessed the magnesium primary production technologies [7]. They identified the most important problem of the electrolysis process to be the enhancement of cell throughput by improvements in mass transport. This fact is in corroboration with the observation made by Richardson, namely that electrochemical cells have the lowest processing rates (time/space yields) of any metallurgical reactor [8]. In fact this aspect had already been identified by Dow in its energy conservation program for magnesium. In a report by Neipert, an improvement in the electrolytic cell efficiency is now the goal of a large research effort [9]. Interestingly, the approach to attaining this goal is to control previously unrecognized process impurities.

One of the major factors affecting energy consumption is the purity of the electrolyte. Boron and sulfur are two species which must be strictly controlled. Boron levels in excess of

10 parts per million are known to decrease cell efficiency; the mechanism of breakdown is a matter of dispute (10). Some feel that boron affects the wettability of magnesium to the cathode; others argue that it prompts coalescence into metal droplets which then detach. Current efficiency can decrease to 50-60%. Sulfate in the amount of several hundred parts per million can also have a major effect on current efficiency and, hence, on energy consumption. The mechanism of degradation is not clear. Some investigators have found that sulfate promotes foaming in the electrolyte; others feel that a passivating film of magnesium oxide and magnesium sulfide forms on the cathode (11). Because the difference in densities between magnesium metal and the molten salt electrolyte is small, small variations in electrolyte circulation can strongly impair the process and reduce current efficiency.

This report describes the results of a study of magnesium electrolysis in the presence of high levels of boron and sulfur.

II. EXPERIMENTAL PROGRAM

The objective of this study was to understand the mechanism of breakdown of all performance in the presence of boron and sulfur impurities. The experimental program involved direct visual observation of magnesium electrolysis under a variety of conditions followed by chemical analysis of the cathodic deposits.

A. PREPARATION OF THE ELECTROLYTE.

The electrolyte composition was chosen to be representative of what is known to be used industrially in anhydrous electrolytic processes: 10% $MgCl_2$, 10% $CaCl_2$, 20% KCl, and 60% NaCl. Throughout this report the term, "uncontaminated," refers to this composition. The effects of boron and sulfur were studied by the addition of 0.05% boron in the form of B_2O_3 and 0.5% sulfur in the form of $MgSO_4$, respectively. The sources of supply and chemical analyses of the various salts and reagents are given in Appendix I.

Before electrolysis, all chloride salts were treated to remove water. $MgCl_2 \cdot 6H_2O$ was heated in vacuum to 170°-200°C for 4-5 hours. The product of this operation was exposed to a flow of 1:1 hydrogen chloride and chlorine gases for 5 hours at 500°C and then purged with argon. $CaCl_2$, KCl and NaCl were treated in much the same fashion except that the vacuum drying step was omitted. After dehydration, salts were handled only in a glove box filled with argon where the moisture content was less than 2 ppm.

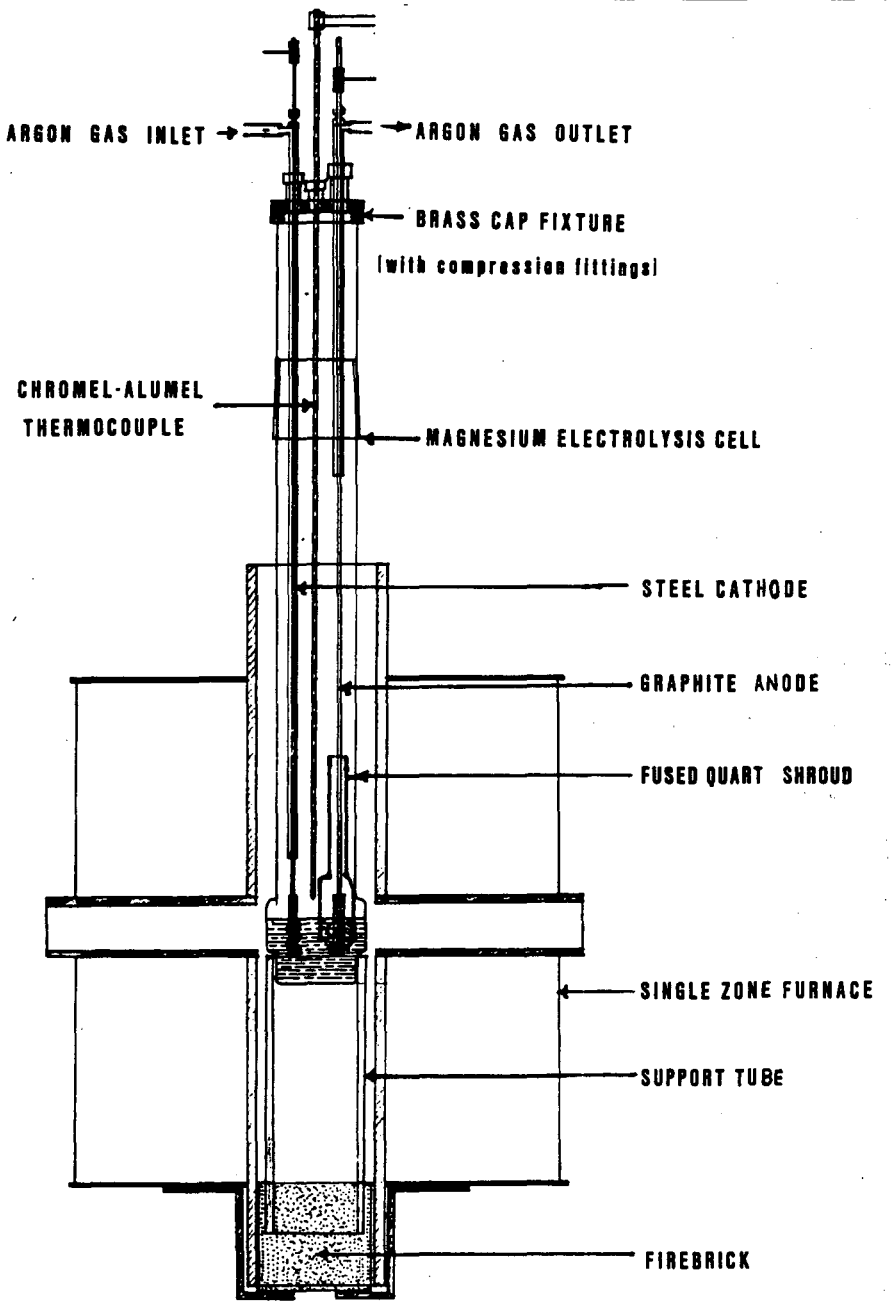

MAGNESIUM ELECTROLYSIS CELL & FIXTURES

Satchit Dokras

MIT

4.1.1982.

CELL AND FURNACE DESIGNS.

The cell electrode system, inert gas system, and the furnace configurations are shown on page 6.

The cell was made of transparent fused quartz that had a 90% transmittance in the IR and visible light regions. At its top was a standard 60/50 tapered male ground glass joint. This was connected to a pyrex female joint onto which a brass cap was sealed with DeKhotinsky cement. The brass cap was water-cooled, and had three ports for an anode, a cathode, and a thermocouple.

The anode rod itself was made of mild steel, and was shrouded by a 10 mm O.D. fused quartz tube which also served as an outlet for the inert gas. At the bottom of this steel rod, a graphite plate (25 mm X 30 mm X 8.5 mm) that actually served as the anodic plate was screwed into place. The gap between this graphite plate, the steel rod, and the fused quartz tube was sealed with graphite cement. This cementing ensured that the electrolyte would at any time be in contact with the anodic graphite alone, and never the steel. The top of the fused quartz tube was sealed with DeKhotinsky cement.

The second port also contained a similar steel rod shrouded by a 10 mm fused quartz tube that served as the inert gas inlet. Its bottom was welded (Tungsten Inert Gas) to a mild steel plate (25 mm X 30 mm X 2 mm) that served as the steel cathode. The top of this fused quartz tube was also

sealed with DeKhotinsky cement.

A fused quartz shroud was placed over both the electrode plates to contain the products of electrolysis. The third port had a thermocouple shrouded in a 6 mm O.D. fused quartz tubing. This was a K-type chromel-alumel thermocouple, and was employed along with an electronic ice point correction unit. The ports had compression fittings in order to seal the cell's contents from the external atmosphere.

The ground glass joint permitted the loading of the cell within the glove box to keep the electrolyte from coming in contact with the moisture in the atmosphere. The joint's seal was made air-tight with silicone grease [1].

Heat was supplied by an electrical resistance furnace [2] with a 3.5 inch tube diameter. It had two diametrically opposed windows of 1 inch diameter at the level of the hot zone. The furnace temperature was controlled by a PID temperature controller [3]. The entire system was seen to maintain a temperature level within ± 2.0 ^{o}C over the dimensions of electrolyte depth.

---

[1] Silicone grease: such as that commercially available under the brand name Corning High Vacuum Silicone Grease.

[2] Electrical resistance furnace: Applied Test Systems Inc., Saxonburg, PA 16056; Series 3100; tube furnace.

[3] PID temperature controller: Athena Controls Inc., West Conshohoken, PA 19428; Series 2100.

B. ELECTROCHEMICAL AND OPTICAL EQUIPMENT

A potentiostat-galvanostat [4] served as power supply for electrolysis at low and medium current densities. At the highest current densities, a power booster [5] was employed.

A single lens reflex 35 mm format camera [6] with a 55 mm f 2.8 macro lens was employed to obtain the photographs within the cell. The light source used was a simple 200 W incandescent light bulb mounted in a reflector. This light source was mounted at a porthole; the camera was mounted at the diametrically opposite porthole.

The entire experimental apparatus - furnace, cell, and optical systems - were mounted atop a pneumatically isolated 6' X 4' optical bench [7].

---

[4] Potentiostat-galvanostat: Aardvark Instruments, Division of Floyd Bell Associates Inc., Columbus, Ohio 43212; Model V-2.

[5] Power booster: Aardvark Instruments; Model X.

[6] Camera: Nikon; Model FE.

[7] Optical bench: Newport Research Corporation, Fountain Valley, CA 92708; Model RS-46-8.

III. EXPERIMENTAL PROCEDURE

Inside the glove box, the salts were weighed on an electronic pan balance and charged into the electrolysis cell. The cell was sealed and transferred from the glove box to the furnace. Electrical, inert gas, and water connections were made and then the salts were carefully melted.

The temperature was manually ramped to 800°C in stages of 100°C over a period of 45 minutes. Another 30 minute period was required at 800°C for the electrolyte to attain homogeneity.

In the meantime, the galvanostat was prepared for the experiment with a dummy cell consisting of a resistance box. The current was set at a particular level and the resistance in the dummy cell fluctuated to ensure that despite changes in the voltage registered there would be no change in the set current level. This done, the anode and cathode leads were connected.

With the cell system ready, the graphite anode was first dipped into the electrolyte and the camera focussed on its surface and kept ready. The galvanostat was then switched on as the steel cathode was quickly dipped into the electrolyte. (This was essential, as if the steel cathode were simply immersed into the electrolyte without an imposed potential, it would have been quickly corroded and would have formed a coating of iron chloride.) Thereafter, as a particular voltage was registered for the ongoing process, photographs were taken with progress in the process and with time.

Upon completion of the experiment, the steel cathode along with its deposit were carefully raised from the electrolyte. The power supply was turned off, the anode and thermocouple lifted

clear of the electrolyte, and the furnace switched off. The system was air-cooled over 8 to 10 hours. Following cooling, the electrode plates were photographed to show the deposit and surface details.

ANALYSIS OF THE ELECTRODEPOSITS.

The analysis of the electrodeposits on the cathode surface was conducted by emission spectrography on an EBERT 3.4 m spectrograph. The sample was crushed in a plastic ball grinder to a -100 mesh size powder and mixed in a 1:9 ratio with graphite. This sample was then compared in its spectrum with standard SQ powder (a semi-quantitative powder with 48 different elements) at the different elemental levels of 1, 10, 100, and 1000 ppm. The comparison was made to determine the sample's concentration as well as range. The photographic plates were read on a densitometer. Sulfur and oxygen contents were specifically analyzed by a LECO instrument capable of detecting their concentrations by infrared detection techniques.

The boron-containing deposit was analyzed by the ESCA or Electron Spectroscopy for Chemical Analysis technique, details of which are provided in APPENDIX II. The electrodeposits were rinsed in distilled water to wash off the adhering chlorides, and to yield a contrast in the ESCA analyses.

IV. RESULTS AND DISCUSSION

To observe the effect of boron and sulfur impurities, magnesium was deposited from electrolytes containing controlled amounts of each contaminant. The effect of current density was also studied. The results were compared to those obtained in "uncontaminated" melts free of these impurities.

The results are presented below, first for the uncontaminated, then for boron and sulfur contaminated, electrolytes, and are discussed individually. Following this, a comparative analysis is made between the contaminated and uncontaminated systems.

A. UNCONTAMINATED ELECTROLTYE.

The voltages registered at the three current density levels for the uncontaminated electrolyte are recorded in Table I. This table also correlates the photographs of the electrodeposition process with the different current density regimes.

TABLE I
Data recorded during electrolysis of uncontaminated electrolyte.

Current Density	Potential with respect to chlorine electrode	Figure
5.55 mA/cm^2	2.6 V	1
27.75 mA/cm^2	2.9 V	2
83.25 mA/cm^2	2.9 V	3

Sabirov et al.[12] studied impurity effects in magnesium chloride melts. They used an electrolyte composition of 90% $MgCl_2$, 5% NaCl, 5% KCl with a steel cathode. Figure 4 shows their polarogram of the uncontaminated melt, as well as with different levels of boron impurity additions. While the composition of their electrolyte differs from those used in the present study, the polarogram is useful in identifying potential electrolysis products.

As can be seen from Figure 1, at low current density chlorine began to form at the anode (at right) with time, and the bubbles grew in size, eventually to detach and to float off; other chlorine bubbles began to form at the anode surface thereafter. The cathode surface was slightly blurred, and the magnesium globules here can be distinguished primarily on the bottom surface of the cathode. These formed, grew, detached, and floated off, too; the same was observed along the vertical cathode surfaces.

In the medium current density regime (27.75 mA/cm^2), Figure 2, the sizes of the chlorine bubbles and the magnesium globules increased rapidly. Their rates of formation, growth, and detachment also increased.

Finally, at the high current density (83.25 mA/cm^2), Figure 3, the reaction rates proved to be excessively vigorous. Even in the initial stages, the chlorine bubbles that formed were huge, and with their rapid formation and detachment, they quickly created a convection current, which eventually was strong enough to pull the deposited magnesium off the cathode. This metal appeared to be drawn toward the anode, and "streamers" were seen to emanate

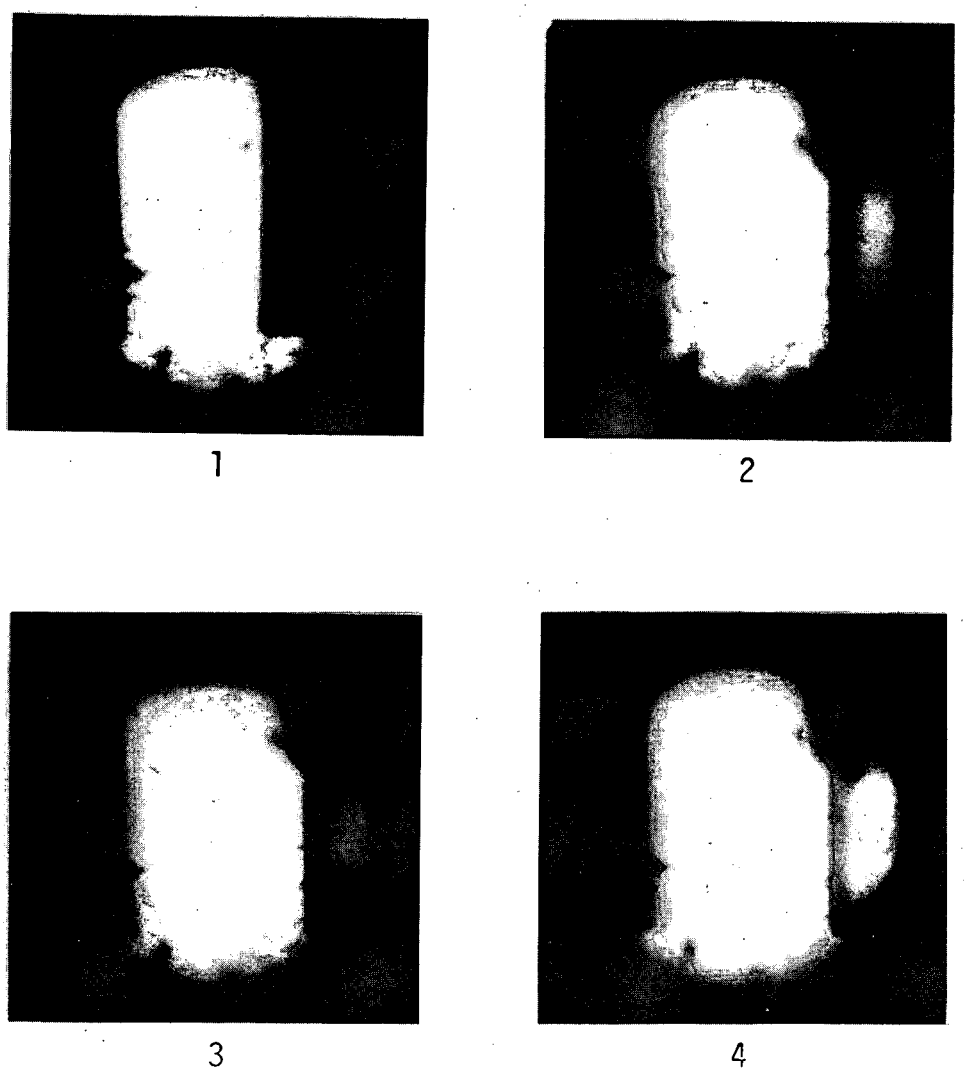

Figure 1. Electrodeposition of magnesium (left) and emanation of chlorine (right) during electrolysis of uncontaminated 10% $MgCl_2$, 10% $CaCl_2$, 20% KCl, 60% NaCl electrolyte at low current density of 5.55 mA/cm^2. Potential with respect to chlorine electrode = 2.6 V. Temperature 800°C.

XBB 842-1462

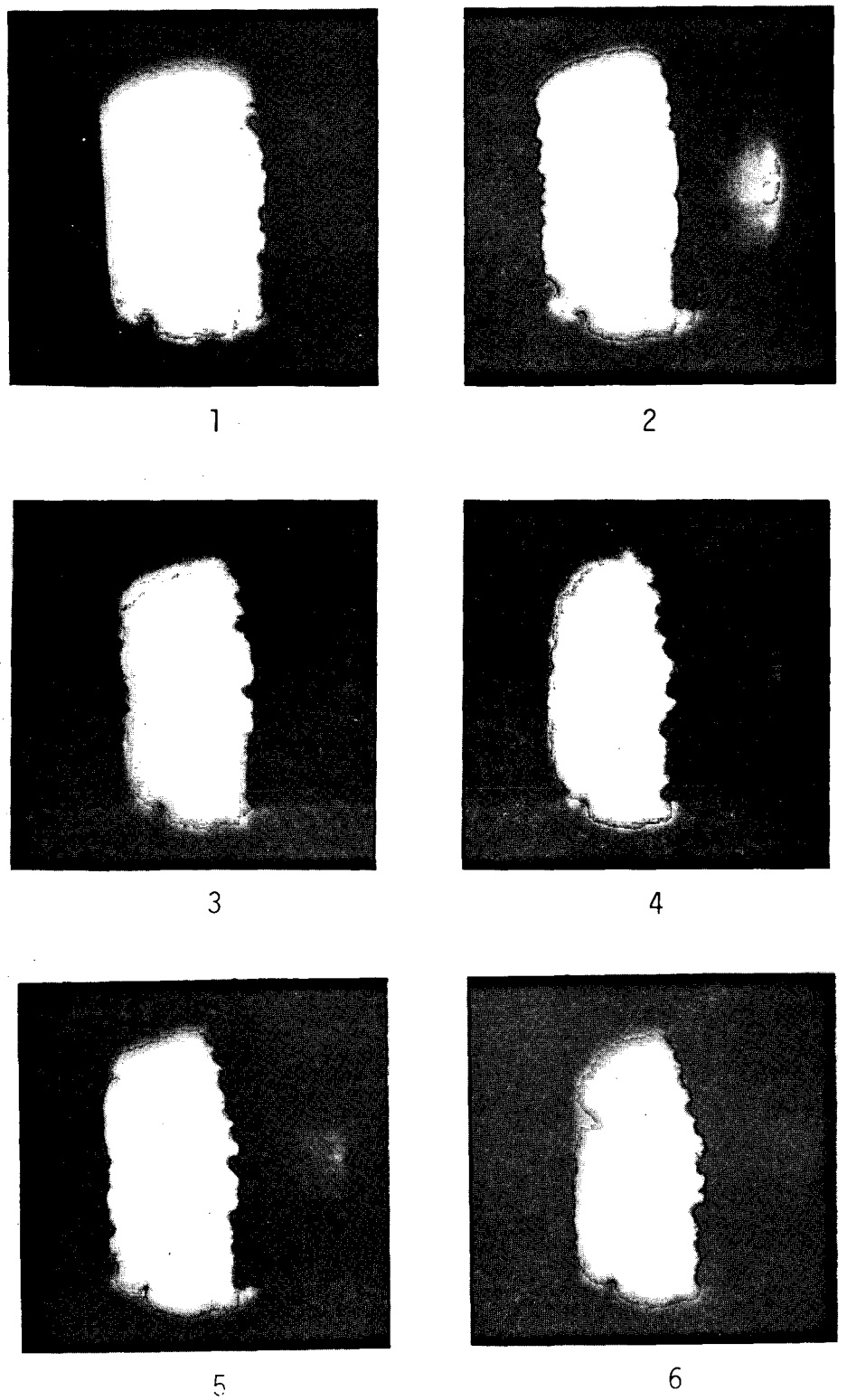

Figure 2. Electrodeposition of magnesium (left) and emanation of chlorine (right) during electrolysis of uncontaminated 10% $MgCl_2$, 10% $CaCl_2$, 20% KCl, 60% NaCl electrolyte at medium current density of 27.75 mA/cm^2. Potential with respect to chlorine electrode = 2.9V. Temperature 800°C.

XBB 842-1461

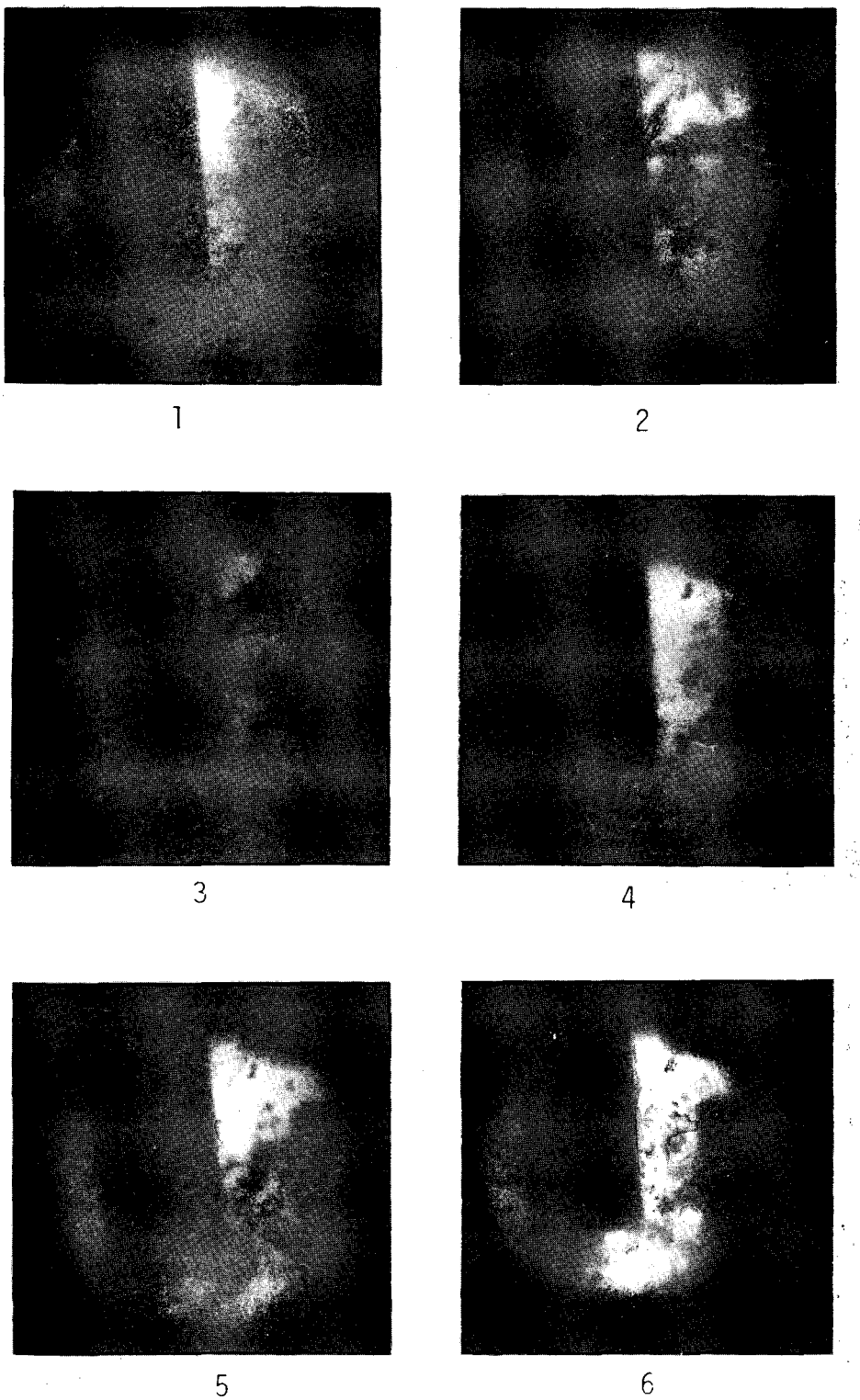

Figure 3. Electrodeposition of magnesium (left) and emanation of chlorine (right) during electrolysis of uncontaminated 10% $MgCl_2$, 10% $CaCl_2$, 20% KCl, 60% NaCl electrolyte at high current density of 83.25 mA/cm^2. Potential with respect to chlorine electrode = 2.9V. Temperature 800°C.

XBB 842-1460

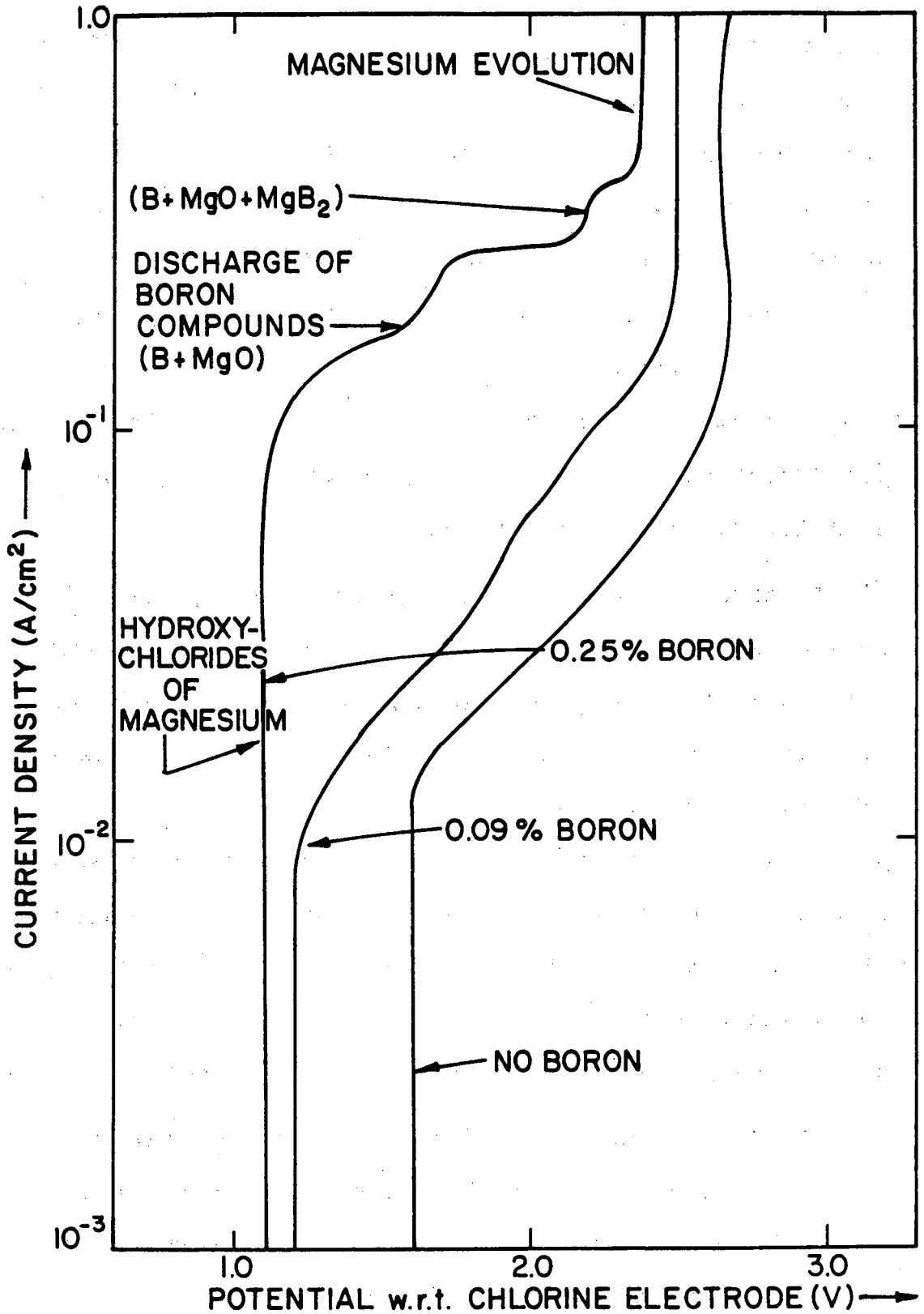

Figure 4. Polarogram of 90% $MgCl_2$, 5% NaCl, 5% KCl melt with boron impurity additions. (Sabirov, et al.[12])

from the cathode. The length of these streamers varied with time: they were seen to form, to grow, and cross the inter-electrode space. In their wake, others formed at other locations on the cathode surface. The density of these streamers increased with time and the electrolyte solution became so occluded as to be virtually opaque (Figure 3, Frame 5). A similar "fog" generated by these streamers is known to emanate from the cathode during the electrolytic production of aluminum from molten cryolite, which is normally clear and transparent [13].

In addition, the voltage was seen to fluctuate in consonance with the streamer development. The streamers were definitely not continuous molten metal that short-circuited the electrode to result in voltage fluctuations. Rather, the streamers appeared to be small clouds of possibly molten metal plucked off the cathode. The highly conductive metal droplets were mechanically mixed (not dissolved) in the molten salt electrolyte which had a much lower electrical conductance. Fluctuations in the position of the metal fraction caused fluctuations in the cell voltage.

TABLE II shows the emission spectography semi-quantitative analysis of the cathodic deposit obtained after the uncontaminated electrolyte was electrolyzed at a medium current density of 27.75 mA/cm^2.

Besides the trace elements belonging to the mild steel cathode, an inordinately large quantity of sodium presence was also evident. However, it has been shown by Zhurin[14] that if the cathodic current density is 0.5 mA/cm^2 or less, the current yield of magnesium decreases strongly if the $MgCl_2$ content in the electrolyte is lower than 7-8 wt %; in such an event, sodium or potassium electrodeposit along with magnesium, depending upon the composition of the electrolyte.

Table II

Semi-quantitative analysis of cathodic deposit of uncontaminated melt at 27.75 mA/cm^2.

Method of analysis: Emission spectrography. Comparative standard: Standard SQ powder at different elemental levels of 1, 10, 100, and 1000 ppm. Analysis procedure: According to standard ASTM recommendations [Ref. 15].

Al	0.001 to 0.01%
Ca	0.1 to 1.0%
Cr	0.001 to 0.01%
Cu	0.0001 to 0.001%
Fe	1.0 to 10.0%
Mg	greater than 10%
Mn	0.01 to 0.1%
Na	greater than 10.0%
Ni	0.0001 to 0.001%
Si	0.0001 to 0.001%

During the course of the present experiment the $MgCl_2$ concentration surely dropped below this level of 7-8 wt.%. It seems that the sodium observed in the cathodic deposit could have codeposited along with the magnesium.

B. ELECTROLYTE WITH BORON CONTAMINATION.

Boron in the form of B_2O_3 was added to the electrolyte to a concentration of 0.05%. Table III reports the voltages registered at the three current densities for this electrolyte and cites the figures containing the corresponding electrodeposition photographs.

TABLE III
Data recorded during electrolysis of boron-contaminated electrolyte.

Current Density	Potential with respect to chlorine electrode	Figure
5.5 mA/cm^2	0.6 V	5
27.75 mA/cm^2	0.9 V	6
83.25 mA/cm^2	-	-

Judging from the potential levels observed by Sabirov *et al.*[12], the regimes of deposition products depend upon the current densities employed (Figure 4). In their study, conducted with a 90% $MgCl_2$, 5% NaCl, 5% KCl electrolyte, at lower current densities (the values actually depend upon the contamination levels of boron within the melt) hydroxychlorides of magnesium were deposited; at still higher current densities, boron discharged with nucleation on the cathode of the elementary compounds of boron and magnesium oxide

(the boron alloys with steel to form iron boride, FeB_2); at still higher levels of current density (and hence potentials), in addition to the above deposits, MgB_2-type compounds also deposit; finally, at the highest current density levels, magnesium begins to evolve at potentials of 2.3 to 2.5 V (depending on boron impurity level). Thus, boron depolarizes magnesium evolution by approximately 0.20 V.

The series of photographs of the boron-contaminated melt electrolyses in Figures 5 and 6 at low and medium current densities, respectively, shows that the cathode is passivated. Thus, the deposition of magnesium is now impeded and a layer of some other substance coats the entire cathode surface. The electrodeposits were subjected to a semi-quantitative emission spectrography analysis, the results of which are shown in Tables IV and V for low and medium current densities, respectively.

The emission spectrography technique was found to be incapable of detecting the presence of boron. To further analyze the deposits, ESCA was done. This technique has the advantage of yielding valuable information on the relative amounts of the individual elements present. However, the emission spectrography results do reveal an excessive amount of sodium , and by virtue of the fact that $MgCl_2$ levels would have fallen below the 7-8% levels, and by the Zhurin report [14], it can be deduced that sodium could have been codeposited along with magnesium.

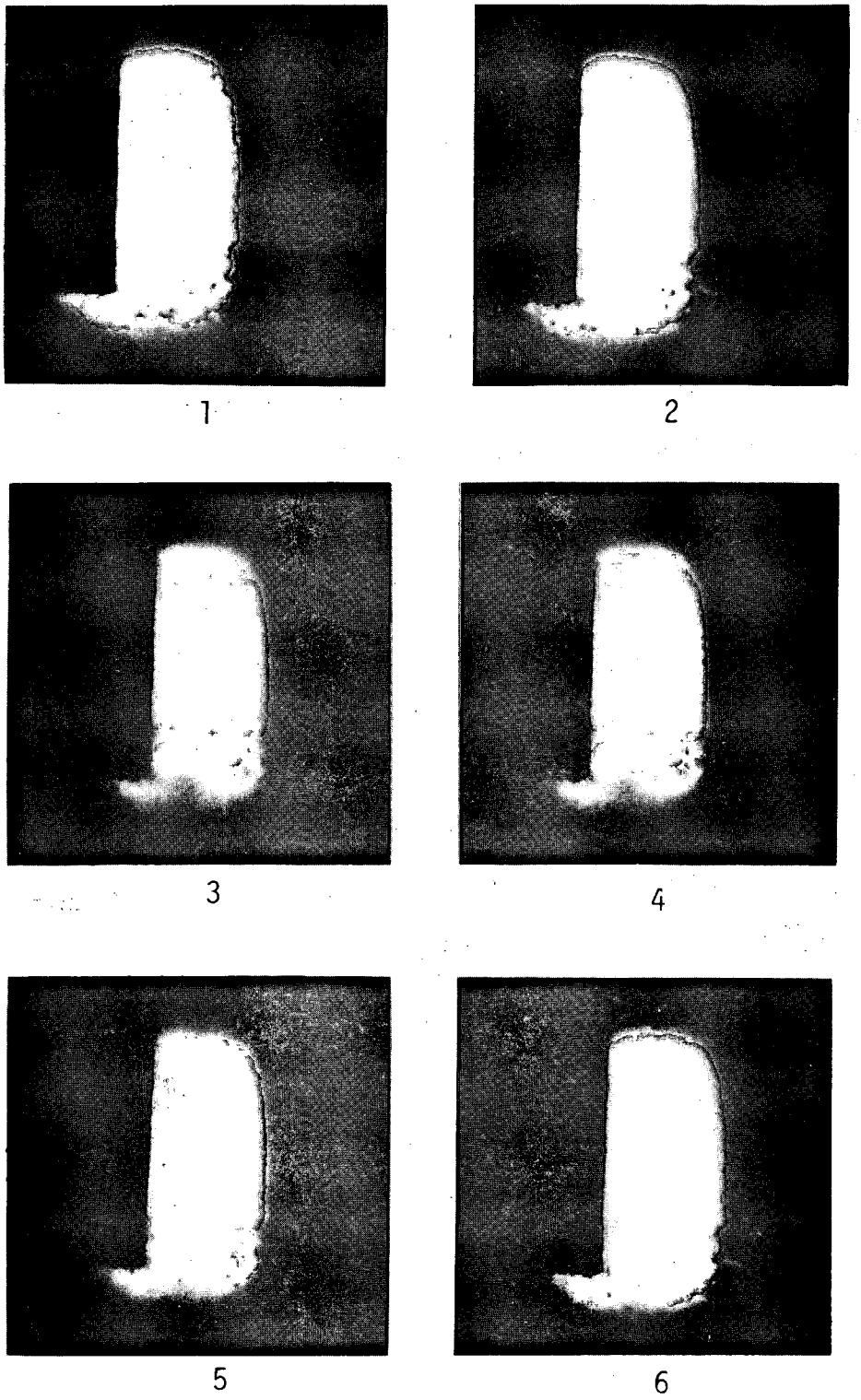

Figure 5. Passivation of cathode (right) with chlorine emanation on anode (left) at low current density of 5.55 mA/cm^2 in a 10% $MgCl_2$, 10% $CaCl_2$, 20% KCl, 60% NaCl electrolyte with 0.05% boron impurity. Potential with respect to chlorine electrode = 0.6 V. Temperature 800°C.

XBB 842-1459

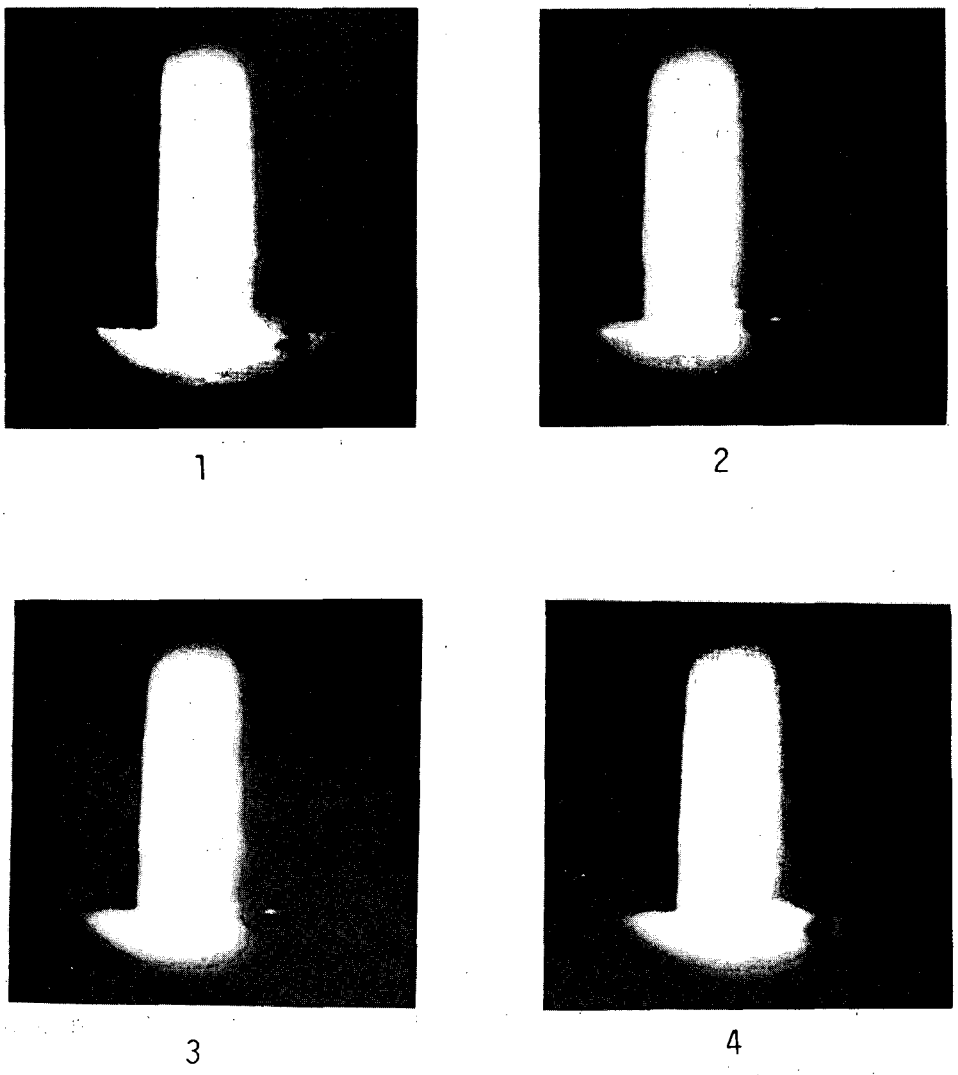

Figure 6. Passivation of cathode (right) with chlorine emanation on anode (left) at medium current density of 27.75 mA/cm^2 in a 10% $MgCl_2$, 10% $CaCl_2$, 20% KCl, 60% NaCl electrolyte with 0.05% boron impurity. Potential with respect to chlorine electrode = 0.9 V. Temperature 800°C.

XBB 842-1458

Table IV

Semi-quantitative analysis of cathodic deposit of boron-contaminated electrolyte at 5.55 mA/cm^2.

Method of analysis: Emission spectrography. Comparative standard: Standard SQ powder at different elemental levels of 1, 10, 100 and 1000 ppm. Analysis Procedure: According to standard ASTM recommendations [Ref. 15].

Al	0.0001 to 0.001%
Ca	0.1 to 1.0%
Cr	0.0001 to 0.001%
Cu	0.0001 to 0.001%
Fe	1.0 to 10.0%
Mg	0.1 to 1.0%
Mn	0.001 to 0.01%
Na	greater than 10%
Ni	0.0001 to 0.001%
Si	0.0001 to 0.001%

Table IV and Appendix II-A present the ESCA analysis for the electrodeposit before the electrode was washed. It was suspected that the results would reflect the composition of the electrolyte to a great extent, and this is indicated in the ratios of Na:Cl being 1:1. B:O = 1:1.52 implies a possibility of B_2O_3 presence. NaCl and B_2O_3 are the constiteunts of the electrolyte itself. Thus, to remove adhering electrolyte from the cathodic deposit, it was rinsed thoroughly with distilled water. Specimens of the electrode film were then analyzed as before by ESCA, and the results are shown

Table V

Semi-quantitative analysis of cathodic deposit of boron-contaminated electrolyte at 27.75 mA/cm^2.

Method of Analysis: Emission spectrography. Comparative standard: Standard SQ powder at different elemental levels of 1, 10, 100, and 1000 ppm. Analysis Procedure: According to standard ASTM recommendations [Ref. 15].

Al	0.0001 to 0.001%
Ca	0.1 to 1.0%
Cr	0.0001 to 0.001%
Cu	0.0001 to 0.001%
Fe	1.0 to 10.0%
Mg	0.1 to 1.0%
Mn	0.001 to 0.01%
Na	greater than 10%
Ni	0.0001 to 0.001%
Si	0.001 to 0.001%

Table VI

Area sensitivities in atomic percent given by ESCA tests on boron-contaminated electrodeposit BEFORE water wash.

Na	29.3
Mg	3.5
B	15.4
Cl	28.5
O	23.4

Table VII

Area sensitivities in atomic percent given by ESCA tests on boron-contaminated electrodeposit AFTER water wash.

Na	7.7
Mg	14.4
B	4.0
Cl	3.1
O	70.7

in Table VII and Appendix II.B.

These data suggest the following:

4 % B: 14.4 % Mg indicates a possibility of MgB_x presence.

70.0 % O : 14.4 % Mg indicates a possibility of MgO presence.

3.1 % Cl : 14.4 % Mg indicates a possibility of some $MgO_xH_yCl_z$-type compound.

Thus, magnesium may be present as MgB_x, MgO, or $MgO_xH_yCl_z$ compounds. But it is definitely not present as $MgCl_2$, as this would have been dissolved away with the water rinse. The techniques of analysis were unable to determine the exact magnesium compounds that had formed.

There is definitely a high percentage of sodium present in the electrodeposit, and this cannot be from NaCl. The quantities of Na and Cl decreased dramatically after the water rinse to indicate that NaCl was dissolved away. The inference that can be made here is that this sodium is present as either Na_2O or in the codeposited form as $MgNa_xB_y$. The previously cited Zhurin study [14] seems to indicate the latter to be more probable, as the $MgCl_2$ levels would have definitely reached below the 7-8% level during electrolysis. However, it was not possible to identify the precise compounds of either Na or Mg with the analysis techniques employed.

Finally, there is an extremely large amount of oxygen present. It is expected that the greater part of this is compounded with iron. However, atmospheric oxygen could also contribute to such a high reading. The ESCA tests could not resolve this.

Thus, on the basis of the chemical analyses performed, the deposit consisted of one or more of the following: MgB_x, MgO, Na_2O, $MgO_xH_yCl_z$, and $MgNa_yB_z$. With the techniques at our disposal it was not possible to identify the precise chemical formulae of the compounds present or their relative concentrations.

At the anode, the chlorine liberation was again observed to be proportional to the current density. It was felt that electrolysis at higher current densities (83.25 mA/cm^2) would not have been sustained by the present system because the vigor of the reaction at the anode, i.e., chlorine liberation, would wipe the cathodic products off the electrode, creating streamers that would short-circuit the cell.

C. ELECTROLYTE WITH SULFUR CONTAMINATION.

The addition of 0.5% sulfur to the electrolyte was made in the form of anhydrous magnesium sulfate. Table VIII reports the voltages registered at the current density levels for this electro lyte and cites the figures containing the corresponding process photographs.

Table VIII
Data recorded during electrolysis of sulfur-contaminated electrolyte.

Current Density	Voltage with respect to chlorine electrode	Figure
5.5 mA/cm^2	0.65 V	7
27.75 mA/cm^2	1.10 V	8
83.25 mA/cm^2	-	-

Direct decomposition of $MgSO_4$ by electrolysis is not very likely owing to its high decomposition voltage (3.4 V at 700°C, Strelets [Ref. 16], p. 240), and to the fact that the concentration of this sulfate is very low. The possible reactions in such a case are:

$$Mg^{2+} + 3\ Mg + SO_4^{2-} = 4\ MgO + S$$

$$Mg^{2+} + 4\ Mg + SO_4^{2-} = 4\ MgO + MgS$$

When these reactions occur, magnesium is lost by the deposition of magnesium oxide on the cathode, with subsequent separation of finely dispersed magnesium.

Ukshe et al. [17],[18] reported that high sulfur concentrations of 0.4 to 0.8% in magnesium salts formed a passivating film of magnesium oxide and magnesium sulfide. This prevents the formation of large drops of magnesium at the cathode, and so increases its polarization. Thus, the current yield shows a considerable decrease.

Strelets [16], p 240 states that the effect of sulfates on the current yield may also be due to the fact that they promote the formation of a consistent foam in which magnesium is entrained in the anodic space.

Figures 7 and 8 show that the optical clarity of the sulfur-bearing electrolyte is poor. It was not possible to determine if this was due to foaming. However, the cathode surface was seen to be passivated, with the result that magnesium metal was not deposited. Chlorine bubbles continued to form on the anode surfaces.

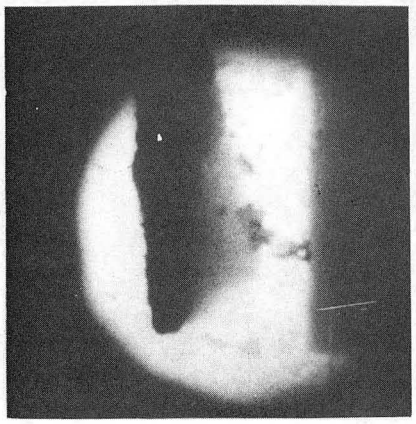

1

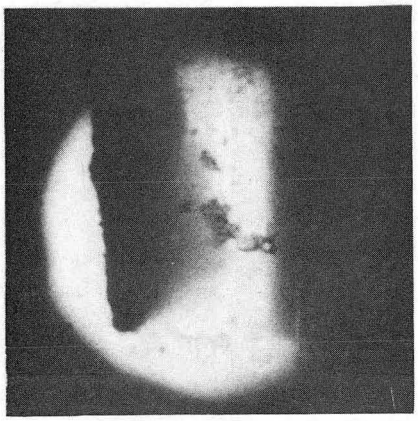

2

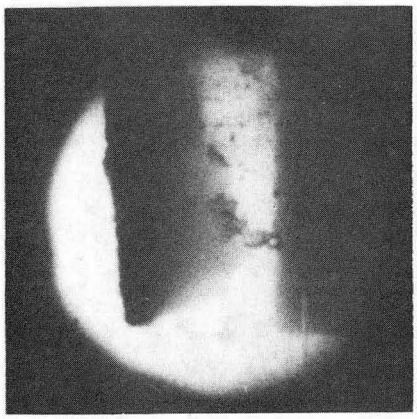

3

Figure 7. Passivation of cathode (left) at a low current density of 5.55 mA/cm^2 in a 10% $MgCl_2$, 10% $CaCl_2$, 20% KCl, 60% NaCl electrolyte with 0.5% sulphur impurity additions. Potential with respect to chlorine electrode = 0.65 V. Temperature 800°C.

XBB 842-1457

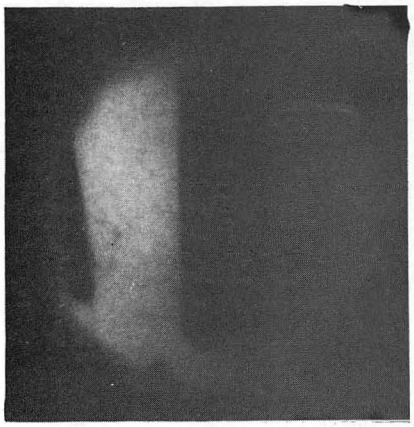

1

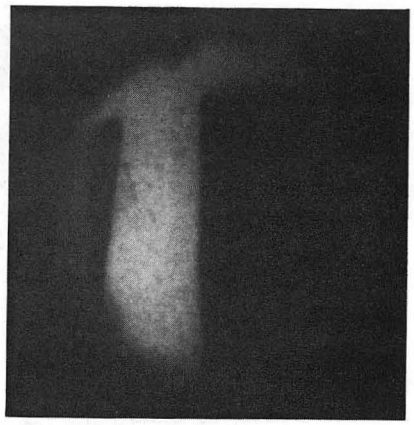

2

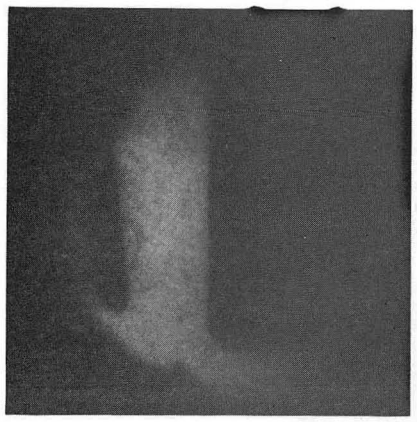

3

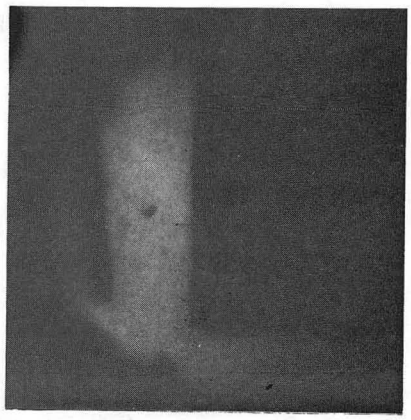

4

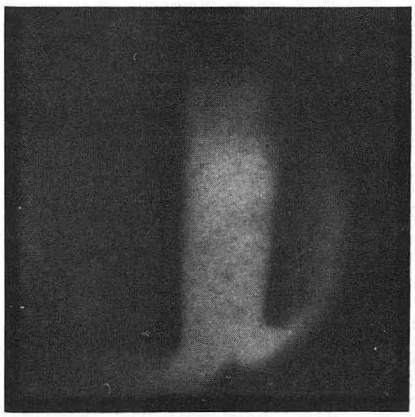

5

Figure 8. Passivation of cathode (left) at a medium current density of 27.75 mA/cm^2 in a 10% $MgCl_2$, 10% $CaCl_2$, 20% KCl, 60% NaCl electrolyte with 0.5% sulfur impurity additions. Potential with respect to chlorine electrode = 1.1 V. Temperature 800°C.

XBB 842-1456

The cathode was subjected to semiquantitative analyses by emission spectrography and infrared detection. The results are given in Table IX.

Again, the results are consistent with sodium codeposition. Magnesium is present in the form of MgO or MgS.

Table IX

(a) Semi-quantitative analysis of cathodic deposit of sulfur-contaminated electrolyte at 27.75 mA/cm^2.

Method of Analysis: Emission spectrography. Comparative Standard: Standard SQ powder at different elemental levels of 1, 10, 100, and 1000 ppm. Analysis Procedure: According to standard ASTM recommendations [Ref. 15].

Al	0.001 to 0.01%
Ca	0.1 to 1.0%
Cr	0.001 to 0.01%
Cu	0.0001 to 0.001%
Fe	1.0 to 10.0%
Mg	greater than 10.0%
Mn	0.01 to 0.1%
Na	greater than 10.0%
Ni	0.001 to 0.01%
Si	0.001 to 0.01%

(b) LECO INFRARED DETECTION ANALYSIS RESULTS:

S	6.55%
O	22.3%

As for the cathodic deposition, the electrolysis of the uncontaminated electrolyte left a smooth cathode surface that appeared unaltered through the experiment. This is consistent with the production of magnesium metal that detached and floated away. In contrast, electrolysis of a boron-bearing electrolyte left a thick deposit over the entire cathode surface, as shown in Figure 9, frame 1. This deposit consisted of many layers which included inorganic compound crusts and entrapped electrolyte. The layers could easily be peeled off. On the basis of the analyses conducted, it is suspected that the deposit could contain some or all of MgB_x, MgO, $MgO_xH_yCl_z$, and $MgNa_xB_y$.

On the other hand, electrolysis of a sulfur-bearing electrolyte produced at the cathode an extremely thin deposit, as seen in Figure 9, frame 2. This deposit peeled off fairly readily. On the basis of the analyses performed, it is suspected that this deposit consisted of magnesium oxide and magnesium sulfide.

Finally, when the uncontaminated electrolyte was electrolyzed at high current densities, streamers were present. After this run, the cathode surface was seen to be totally corroded and seemed to have a granular texture. It appears that the chlorine gas produced at the anode was convectively transported to the cathode and caused the corrosion. The green and orange tinges of iron chlorides were discernible on the cathode surface.

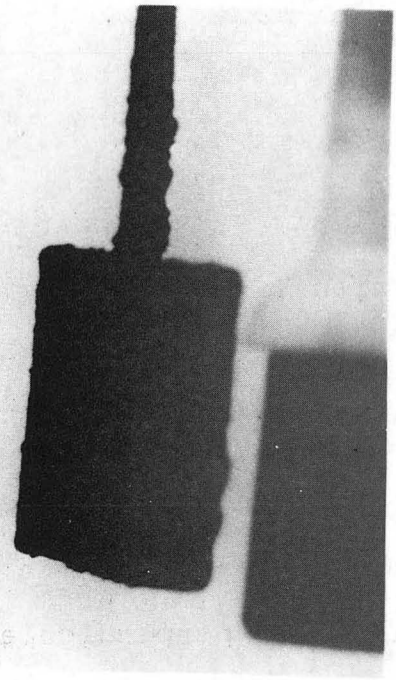

(1)

(2)

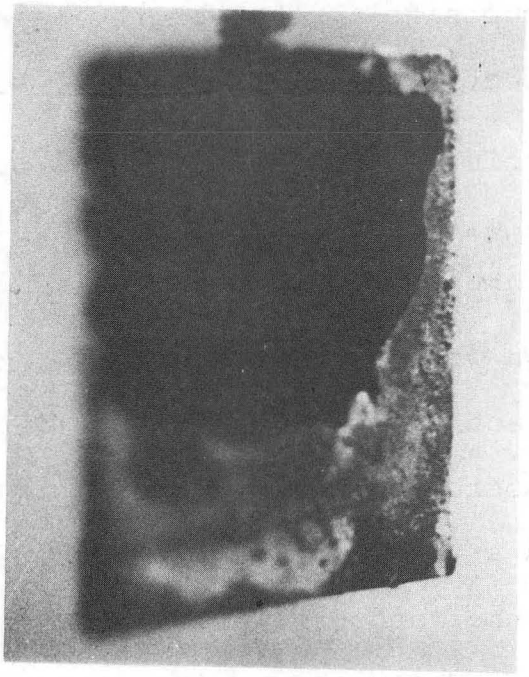

(3)

Figure 9. The electrodeposit on the cathodic surface: (1) with boron impurity; (2) with sulfur impurity; and (3) in uncontaminated electrolyte, at a high current density of 83.25 mA/cm^2.

XBB 842-1455

V. CONCLUSIONS.

THE EXPERIMENTAL TECHNIQUE:

A laboratory scale electrolysis system that is representative of the industrial conditions, and that permits visual observation within the electrolysis cell has been constructed.

The limitations of the optics lie in the fact that the camera, with its macro lens and very narrow depth of field, can focus on only one plane that lies perpendicular to the electrode surface. Thus, the entire electrode surface is not scanned fully in any single instance. Besides, as the light source is opposite to that of the camera, it is possible to capture the electrode and deposit only as silhouettes.

A possible solution to the above two problems is to procure a furnace with three portholes, two diametrically opposite to each other, and one at a 30° angle to one of these. This design would permit one to illuminate and to photograph the electrode from the same side. However, the diametrically opposite porthole employed in the present study facilitates a Schlieren study of the electrolyte motion. Once passivated, the cathodes were inactive under study by simple photography. Under these circumstances, it is felt that Schlieren imaging of the electrolyte flow should be informative.

Finally, it is necessary to reach higher current densities to study the entire range of the electrodeposition process for a particular melt composition. The electrode dimensions could be reduced to attain this.

THE EXPERIMENTAL RESULTS:

The mechanism of electrodeposition of magnesium is the nucleation of a molten metal droplet on the cathode surface. The droplet grows until it becomes large enough to overcome the forces of surface tension, whereupon it detaches from the cathode and floats to the electrolyte surface. The greater the current density, the larger are the globules formed, and the faster is their rate of growth and detachment. However, at very high current densities, the rate of reaction is so vigorous that the magnesium streamers emanating from the cathode extend all the way across to the anode, and the chlorine bubbles are in turn circulated as far as to the cathode. This promotes the so-called back reaction of magnesium and chlorine , and causes corrosion of the mild steel cathode by chlorine. As mentioned before, the size (controlled probably by the electrostatic and hydrodynamic effects) and growth rate of the chlorine bubbles are proportional to the current density.

The presence of boron at 0.05% levels in the melts prevents the formation of any elemental magnesium at the cathode at low and medium current densities; instead, it is

suspected that some forms of magnesium compounds with chlorine, oxygen, boron and sodium are formed which coat the cathode, thereby passivating it. Similarly, at low and medium current densities, the presence of 0.5% sulfur in the melt prevents magnesium deposition as possibly magnesium oxide and magnesium sulfide are deposited on the cathode instead, thus rendering this cathode passivated.

LIST OF PUBLICATIONS

S. M. Dokras, "Electrolyte Impurity Effects on Magnesium Electrodeposition," S. M. Thesis, M.I.T., 1983.

ARTICLES IN PREPARATION

S. M. Dokras and D. R. Sadoway, "Electrolyte Impurity Effects on Magnesium Electrodeposition," to be submitted to Metallurgica Transactions.

EVALUATION OF PROGRESS

The technical scope of work was divided into two principal tasks, Task I: electrode configuration, and Task II: electrolyte contamination.

Task II was completed in its entirety. This technical report describes in detail an improved understanding of how boron and sulfur cause magnesium electrolysis cells to malfunction. Task I was only partially completed. It became apparent that the scale of equipment that had been constructed for the electrode contamination studies was too small to permit easy variation of electrode configuration. Consultation with industrial technical staff made it clear that bipolar electrode testing was far more complex than originally anticipated. In spite of this, the transparent cell constructed for the present study permitted *in situ* observation of electrolyte, magnesium metal, and chlorine gas under a wide variety of processing conditions. These results are also described in detail in this technical report.

The light metals have an important role to play in energy conservation, yet research into efficient processing technologies for these materials has been almost totally neglected by American universities. Through this project a new research initiative was begun in this area of light metals processing. In response, domestic light metals producers have shown an interest in supporting further research of this type at M.I.T.

APPENDIX I

PURITY OF SALTS

$MgCl_2$: Analytical reagent grade. MX 0045-1, lot no.12NO7.
Manufacturer: MCB Manufacturing Chemists Inc.
2909 Highland Ave., Cincinnati, Ohio 45212.

$CaCl_2$: Analytical reagent grade. AC-1946. lot no.080410.
Manufacturer: Anachemia Ltd., Champlain, NY 12919.

KCl: Analytical reagent grade. R-282, lot no.713348.
Manufacturer: Fisher Scientific Company, Chemicals Manufacturing Division, Fairlawn NJ 07410.

NaCl: Analytical reagent grade. S-271, lot no.712476.
Manufacturer: Fisher Scientific Company, address as above.

$MgSO_4$: Analytical reagent grade. MX 0075-1, lot no.2P24.
Manufacturer:MCB Manufacturing Chemists Inc.
Address as above.

B_2O_3: Analytical reagent grade 99.99%. 89964, lot no.031582.
Manufacturer: Alfa Products, 152 Andover St., Danvers, MA 01923.

In all cases, analysis meets ACS specifications.

Graphite: Source: Pure CArbon Company Inc., St.Mary's,PA.
Grade: DS-1, resistivity=0.0018 O/cm.

Steel: Source: U S Steel.
Grade: Low carbon steel.

APPENDIX II

ESCA ANALYSIS REPORTS.

Electron Spectroscopy for Chemical Analysis (ESCA) is conducted by irradiating the sample by mono-energetic soft x-rays and energy, and thereby analyzing the electrons emitted. MgK_{α} x-rays (1253.6 eV) are used as the source, and these have the penetrating power in a solid of 1-10 um. ESCA is conducted by first making a survey scan, then a detailed scan for each of the elements of interest, and then finally making an area sensitivity comparison for the atomic ratios in which the elements are present.

Survey Scans: A scan range of 0 to 1000 eV is sufficient for the identification of all detectable elements.

Detail Scans: For purposes for chemical state identification, for quantitive analysis of minor components and for peak deconvolutions, and for other mathematical manipulations of the data, detailed scans must be obtained for precise peak locations and for accurate registration of line shapes.

Quantitative Analysis: For quantifying the ESCA measurements, peak area sensitivities were used.

Reference: Handbook of X-Ray Photoelectron Spectroscopy, ed.G.E.Muilenberg, pub.Perkin-Elmer Corporation, Minnesota.

BIBLIOGRAPHY

1. R. O. Loutfy, R. L. Leroy, J. Appl. Electrochem., 8 (1978), p. 549-555.

2. G. B. Kenney, J. P. Clark, "An Overview of Energy Conservation by Substitution of Magnesium for Other Metals," Report at Intl. Conf. on Energy Conservation in Production and Utilization of Magnesium, MIT, May 1977.

3. S. Rabinowitz, "Magnesium in Automotive Castings," Proc. of 32nd Annual Meeting of International Magnesium Association, May 1975.

4. D. G. Adams et al., "Charger XL: A Lightweight Materials Development Vehicle," SAE Paper No. 760203.

5. G. B. Kenney, "An Analysis of the Energy Efficiency and Economic Viability of Expanded Magnesium Utilization," Sc.D. Thesis, MIT, 1979.

6. M. C. Flemings, G. B. Kenney, "Materials Substitution and Development for Light Weight, Energy Efficient Automobile," Report to OTA, U. S. Congress, Feb. 8, 1980.

7. M. C. Flemings, D. R. Sadoway, G. B. Kenney, J. P. Clark, J. Szekeley, "Am Assessment of the Magnesium Primary Production Technology," Report to DOE, Feb. 1, 1981.

8. F. D. Richardson, Trans. Inst. Min. Metall., 84A (1975), p. 19-25.

9. M. P. Neipert, "Dow's Energy Conservation Program for Magnesium," Proc. of World Annual Conference on Magnesium, Salt Lake City, June 8-11, 1980, p. 30.

10. P. P. Fedot'ev, Elektroliz v metallurgii, Khimteor etizdat, Moscow, 1934.

11. Trudy Nisalyuminiya, No. 10 (1935), p. 19.

12. Kh. Kh. Sabirov, N. V. Bondarenko, N. N. Gurinovich, Zh. Prikl. Khim. (Leningrad), 51 No. 7 (1978), p. 1572-75.

13. A. Vajna, Bull. Soc. France Elektriciens, 14 (1952), p. 93.

14. A. I. Zhurin, O. G. Destyanikov, Tr. Leningr. Politekh. Inst., No. 1 (1946), p. 279.

15. ASTM Methods for Emission Spectrochemical Analysis, 1968 edition, pub. ASTM, Philadelphia.

16. Kh. L. Strelets, Electrolytic Production of Magnesium, Izdatel'stvo "Metallurgia," Moscow, 1972.

17. E. A. Ukshe, S. A. Pushkareva, Dokl. AN SSSR, 4 No. 2 (1950), p. 370.

18. E. A. Ukshe, S. A. Stepanov, Zh. Fiz. Khim., 34 No. 3 (1960), p. 559.

This report was done with support from the Department of Energy. Any conclusions or opinions expressed in this report represent solely those of the author(s) and not necessarily those of The Regents of the University of California, the Lawrence Berkeley Laboratory or the Department of Energy.

Reference to a company or product name does not imply approval or recommendation of the product by the University of California or the U.S. Department of Energy to the exclusion of others that may be suitable.

TECHNICAL INFORMATION DEPARTMENT
LAWRENCE BERKELEY LABORATORY
UNIVERSITY OF CALIFORNIA
BERKELEY, CALIFORNIA 94720